IAWA Journal, Vol. 26 (2), 2005: 175–187

ESTIMATION OF MICROFIBRIL ANGLE AND STIFFNESS BY NEAR INFRARED SPECTROSCOPY USING SAMPLE SETS HAVING LIMITED WOOD DENSITY VARIATION

Laurence R. Schimleck[1], Robert Evans[2], P. David Jones[1], Richard F. Daniels[1], Gary F. Peter[3] & Alexander Clark III[4]

SUMMARY

Near infrared (NIR) spectroscopy offers a rapid method for the estimation of microfibril angle (MFA) and SilviScan-estimated wood stiffness ($E_{L(SS)}$). The success of these NIR calibrations may be related to air-dry density, because density varies in wood simultaneously with MFA and stiffness. The importance of density variation was investigated by developing calibrations for MFA and $E_{L(SS)}$ using *Pinus radiata* D. Don (radiata pine) and *Pinus taeda* L. (loblolly pine) sample sets where the density range was small and the relationships between density and MFA and density and $E_{L(SS)}$ were poor. Excellent calibrations for MFA and $E_{L(SS)}$ were obtained, particularly when sets had densities greater than 500 kg/m^3, demonstrating that NIR spectroscopy can provide strong relationships for MFA and stiffness even when density variation is limited. Examination of loading plots from the MFA and $E_{L(SS)}$ calibrations indicates that variation in wood components such as cellulose, lignin and possibly hemicellulose is important.

Key words: Near infrared spectroscopy, density, microfibril angle, stiffness, *Pinus radiata*, *Pinus taeda*.

INTRODUCTION

Recently, Schimleck and Evans (2002a, b) reported using near infrared (NIR) spectroscopy to predict microfibril angle (MFA) (defined as the angle that the helical windings of cellulose chains, within the fibre wall, make with the fibre axis) and SilviScan-estimated stiffness ($E_{L(SS)}$). In these studies, diffuse reflectance NIR spectra were obtained from the radial-longitudinal face of wooden strips that had been cut from increment cores for SilviScan analysis. NIR spectra were collected from a total of eight *Pinus radiata* D. Don (radiata pine) increment cores in 10-mm sections and used to estimate radial changes in MFA and $E_{L(SS)}$ for two *P. radiata* cores.

1) Warnell School of Forest Resources, The University of Georgia, Athens, GA 30602-2152, USA. – Corresponding author: Laurence Schimleck [lschimleck@smokey.forestry.uga.edu].
2) CSIRO Forestry and Forest Products, Private Bag 10, Clayton South MDC, Victoria, 3169, Australia.
3) School of Forest Resources and Conservation, University of Florida, Gainesville, FL, USA.
4) USDA Forest Service, Southern Research Station, Athens, GA, USA.

Associate Editor: Michael Wiemann

The underlying physiochemical relationships that make it possible to estimate MFA by NIR spectroscopy are unclear. Dissecting these relationships is often confounded because multiple wood and fiber properties vary simultaneously with cambial age. Generally in *Pinus* species, MFA decreases, while density and fiber length increase with cambial age (Zobel & Sprague 1998). Schimleck and Evans (2002b) presented evidence that suggested that variation in cellulose content was an important factor in the success of their MFA calibration. However, in the *P. radiata* calibration set used by Schimleck and Evans (2002b), the relationship between density and MFA was reasonably strong and therefore it is possible that the density–MFA relationship is also an important factor in the success of their MFA calibration.

Recently, using a limited number of *Eucalyptus nitens* (Deane & Maiden) Maiden (Shining gum) samples, Schimleck *et al*. (2003) demonstrated that it was possible to obtain reasonable calibrations for MFA and $E_{L(SS)}$ when these parameters had weak or no relationships with density (coefficient of determination (R^2) density and MFA = 0, R^2 density and $E_{L(SS)}$ = 0.53). The *E. nitens* MFA calibration had a lower R^2 (0.69) than reported for the *P. radiata* calibration (Schimleck & Evans 2002b) and when applied to a separate test set predicted the MFA of samples poorly, while the $E_{L(SS)}$ calibration had a strong R^2 (0.80) and performed well in prediction. The MFA calibration was obtained using samples that had a narrow MFA range (12.0 to 26.8°) and was applied to a prediction set that had an even narrower range (11.6 to 23.3°). The poor performance of the MFA calibration was attributed to the limited MFA range of both the calibration and prediction sets not to the poor density–MFA relationship. The results of this study indicate that it may be possible to obtain strong MFA calibrations with NIR spectroscopy without having to rely on density variation.

Therefore, to understand more about the relationships that make it possible to obtain predictive calibrations for MFA and $E_{L(SS)}$ using diffuse reflectance NIR spectra obtained in 10-mm sections from the radial longitudinal face of wooden strips, we investigated whether it is possible to develop calibrations for MFA and $E_{L(SS)}$ using sample sets where the density range is small and the relationships between density and MFA and density and $E_{L(SS)}$ are poor.

EXPERIMENTAL

Calibration samples

Set 1 – *Pinus radiata*

These samples have been described in Schimleck and Evans (2002a, b). For this study the NIR spectra of the calibration (119, representing 8 cores) and prediction sets (33, representing 2 cores) were combined to give a total of 152 spectra. The samples were taken from breast height in 26-year-old trees, growing on a single site that had been thinned at age fourteen. Five core samples were selected from trees that had been fertilised with nitrogen (200 kg/ha) and phosphorus (100 kg/ha) once after thinning (Nyakuengama *et al*. 2002). The remaining five cores were chosen from trees that had been thinned but not fertilised. The cores were selected from trees that demonstrated different patterns of radial variation in MFA and represented the range of tree breast-height diameters.

Set 2 – *Pinus taeda*

Ninety breast-height (1.30 m) increment cores were collected from nine *Pinus taeda* (loblolly pine) plantations in Georgia, USA. For each of three geographic regions where *P. taeda* is grown (Lower and Upper Atlantic Coastal Plain, and Piedmont) three plantations were sampled. The selected sites had a range of site qualities (low, medium and high). For each site ten trees with a range of breast-height diameters were sampled. A total of 729 NIR spectra representing 89 radial strips were available from this sample set for analysis (one strip could not be analysed by SilviScan and was excluded from the set).

SilviScan analysis – measurement of wood properties

Radial strips for analysis by SilviScan-1 and -2 were cut from the cores using a twin-blade saw. Strip dimensions were 2 mm tangentially and 7 mm longitudinally, radial length was determined by the pith to bark length of the samples.

Wood properties were measured using SilviScan-1 and -2 (Evans 1994, 1997, 1999). Air-dry density (referred to as density in the remainder of the text) was measured in 50-micron steps using X-ray densitometry. MFA was averaged over 1.0-mm intervals on SilviScan-2 using scanning X-ray diffractometry. An estimate of wood stiffness (at the same resolution as MFA) was obtained by combining X-ray densitometry and X-ray diffraction data (Evans 2005). All measurements were made in a conditioned atmosphere maintained at 40% RH and 20 °C. Wood property averages were determined over 10-mm sections for correlation with the NIR spectra.

Near infrared spectroscopy

Diffuse reflectance NIR spectra were obtained from the radial longitudinal face of each core sample using a NIRSystems Inc. Model 5000 scanning spectrophotometer. The instrument reference was a ceramic standard. Samples were held in a custom-made holder (Schimleck *et al*. 2001). A 5 × 10 mm mask was used to ensure a constant area was tested. The spectra were collected at 2 nm intervals over the wavelength range 1100–2500 nm. Fifty scans were accumulated for each 10-mm section, and these scans were averaged to give a single average spectrum per section. All samples were conditioned in an atmosphere maintained at 40% RH and 20 °C prior to NIR analysis.

Calibration development

To minimise density variation within a given *P. radiata* and *P. taeda* calibration set, spectra were sorted based on the average density of each 10-mm section and split into groups of 100 kg/m^3 range, e.g. 400–499.9 kg/m^3, 500–599.9 kg/m^3 etc. For the *P. radiata* 300.0–399.9 kg/m^3 (5 samples), *P. radiata* 700.0–799.9 kg/m^3 (5 samples) and *P. taeda* 800.0–899.9 kg/m^3 (3 samples) sets calibrations were not developed because of insufficient samples. It was observed for the *P. taeda* set that some groups (400–499.9 kg/m^3, 500–599.9 kg/m^3 and 600–699.9 kg/m^3) had over 150 samples available for calibration, hence it was decided to further divide these sets using a density range of 50 kg/m^3. These sets are summarised in Tables 1 (*P. radiata*) and 2 (*P. taeda*).

Table 1. Microfibril angle (MFA) and SilviScan determined stiffness ($E_{L(SS)}$) summary statistics for the *Pinus radiata* calibration sets. The relationships between MFA, $E_{L(SS)}$ and density for each set are also shown. The average and standard deviation of each set is given in parentheses.

Density range (kg/m^3)	Number of samples	MFA range (degrees)	R^2 (MFA and density)	$E_{L(SS)}$ range (GPa)	R^2 ($E_{L(SS)}$ and density)	R^2 (MFA and $E_{L(SS)}$)
400.0–499.9	37	24.7–41.6 (31.6, 4.2)	0.07	2.5–8.1 (5.7, 1.6)	0.35	0.78
500.0–599.9	77	11.3–36.3 (22.2, 5.3)	0.25	4.6–18.1 (11.8, 3.1)	0.41	0.94
600.0–699.9	30	10.7–26.6 (16.9, 3.6)	0.09	9.6–23.9 (16.7, 3.1)	0.22	0.92

Table 2. Microfibril angle (MFA) and SilviScan determined stiffness ($E_{L(SS)}$) summary statistics for the *Pinus taeda* calibration sets. The relationships between MFA, $E_{L(SS)}$ and density for each set are also shown. The average and standard deviation of each set is given in parentheses.

Density range (kg/m^3)	Number of samples	MFA range (degrees)	R^2 (MFA and density)	$E_{L(SS)}$ range (GPa)	R^2 ($E_{L(SS)}$ and density)	R^2 (MFA and $E_{L(SS)}$)
300.0 – 399.9	17	25.9–40.7 (32.8, 4.4)	0.13	2.4–5.3 (3.7, 1.0)	0.31	0.72
400.0–499.9	157	22.3–45.2 (32.6, 4.4)	0.00	2.5–8.6 (4.8, 1.2)	0.13	0.66
500.0–5.99.9	240	13.0–42.2 (28.6, 6.4)	0.07	3.3–16.5 (7.9, 2.99)	0.20	0.88
600.0–699.9	229	11.0–43.0 (23.0, 6.4)	0.04	4.7–20.5 (12.4, 3.6)	0.12	0.94
700.0–799.9	83	11.2–34.1 (18.8, 5.1)	0.02	8.1–23.1 (16.7, 3.5)	0.12	0.92
400.0–449.9	69	24.1–43.1 (33.1, 4.3)	0.01	2.5–7.3 (4.3, 1.0)	0.02	0.73
450.0–499.9	88	22.3–45.2 (32.3, 4.5)	0.02	3.0–8.6 (5.1, 1.2)	0.02	0.69
500.0–549.9	133	16.2–42.2 (29.9, 5.7)	0.01	3.3–13.9 (6.9, 2.2)	0.07	0.86
550.0–599.9	107	13.0–42.1 (26.9, 6.8)	0.02	3.8–16.5 (9.2, 3.1)	0.06	0.94
600.0–649.9	127	11.3–43.0 (24.0, 6.3)	0.00	4.7–18.3 (11.4, 3.3)	0.01	0.94
650.0–699.9	102	11.0–39.4 (21.8, 6.4)	0.03	5.4–20.5 (13.7, 3.6)	0.07	0.97

The spectra were converted to the second derivative mode using Unscrambler software (version 8.0). Left and right gap widths of 8 nm were used for the conversion. The wavelength range was limited to 1108 to 2490 nm for calibration development based on conversion to the second derivative. The calibrations for MFA and stiffness were developed using Partial Least Squares (PLS) regression and the second derivative treated spectra. Calibrations were developed with four cross validation segments.

The Standard Error of Calibration (SEC) (determined from the residuals of the final calibration), the coefficient of determination (R^2) and the ratio of performance to deviation (RPD) (Williams & Sobering 1993), calculated as the ratio of the standard deviation of the reference data to the SEC, were used to assess calibration performance. Determination of the RPD allows comparison of calibrations developed for different wood properties that have differing data ranges, the higher the RPD the more accurate the data fitted by the calibration.

RESULTS

Calibrations for MFA and $E_{L(SS)}$ – P. radiata

PLS regression calibrations for MFA and $E_{L(SS)}$ were generated using the three *P. radiata* sets for which the density range had been limited to 100 kg/m^3. Summary statistics for each calibration are provided in Table 3. These results show that, when the density range has been limited to 100 kg/m^3 and when the relationships between density and MFA and density and $E_{L(SS)}$ are poor, it is still possible to obtain MFA and $E_{L(SS)}$ calibrations (Table 1). MFA and $E_{L(SS)}$ calibrations developed with the lowest density samples (400–499.9 kg/m^3) had the lowest R^2 and RPD. The MFA and $E_{L(SS)}$ calibrations for each set improved as density of the set increased; although, the improvements in the $E_{L(SS)}$ calibrations were small.

The MFA calibration for the 600–699.9 kg/m^3 set had a very small SEC (0.40°), high R^2 (0.99) and high RPD (9.1). Judging by the RPD's reported for the other MFA calibrations it is probable that this calibration was over-fitted. If 3 factors were used for the 600–699.9 kg/m^3 MFA calibration (to be equivalent to the other *P. radiata* MFA calibrations) a R^2 of 0.90 and a RPD of 3.3 were obtained.

Table 3. Summary of Microfibril angle (MFA) and SilviScan determined stiffness ($E_{L(SS)}$) calibrations developed using *Pinus radiata* sets that had a limited density range (100 kg/m^3).

Wood property	Number of factors	R^2	SEC	RPD
400.0–499.9				
MFA	3	0.79	1.9 deg.	2.2
$E_{L(SS)}$	3	0.84	0.6 GPa	2.5
500.0–599.9				
MFA	3	0.86	2.0 deg.	2.6
$E_{L(SS)}$	3	0.85	1.2 GPa	2.6
600.0–699.9				
MFA	6	0.99	0.4 deg.	9.1
$E_{L(SS)}$	2	0.86	1.2 GPa	2.7

Calibrations for MFA and $E_{L(SS)}$ – P. taeda

PLS regression calibrations for MFA and $E_{L(SS)}$ were generated for the five *P. taeda* sets that had their range of densities limited to 100 kg/m^3 and for the six *P. taeda* sets that had their range of densities limited to 50 kg/m^3. Summary statistics for each calibration are provided in Table 4. Note that if MFA and $E_{L(SS)}$ calibrations were developed using all *P. taeda* spectra (729), 6 factor calibrations were recommended by the software for both $E_{L(SS)}$ (R^2 = 0.92 and SEC = 1.39 GPa) and MFA (R^2 = 0.89 and SEC = 2.42 degrees).

Table 4. Summary of Microfibril angle (MFA) and SilviScan determined stiffness ($E_{L(SS)}$) calibrations developed using *Pinus taeda* sets that had a limited density range (100 kg/m^3).

Wood property	Number of factors	R^2	SEC	RPD
300.0–399.9				
MFA	1	0.41	3.4 deg.	1.3
$E_{L(SS)}$	2	0.67	0.6 GPa	1.7
400.0–499.9				
MFA	4	0.55	3.0 deg.	1.5
$E_{L(SS)}$	4	0.57	0.8 GPa	1.5
500.0–599.9				
MFA	5	0.92	2.0 deg.	3.2
$E_{L(SS)}$	6	0.95	0.7 GPa	4.0
600.0–699.9				
MFA	6	0.93	1.7 deg.	3.9
$E_{L(SS)}$	6	0.92	1.0 GPa	3.5
700.0–799.9				
MFA	6	0.96	1.1 deg.	4.9
$E_{L(SS)}$	4	0.88	1.2 GPa	2.9
400.0–449.9				
MFA	3	0.60	2.7 deg.	1.6
$E_{L(SS)}$	3	0.59	0.7 GPa	1.6
450.0–499.9				
MFA	2	0.49	3.3 deg.	1.4
$E_{L(SS)}$	3	0.62	0.8 GPa	1.6
500.0–549.9				
MFA	6	0.87	2.1 deg.	2.8
$E_{L(SS)}$	7	0.91	0.7 GPa	3.4
550.0–599.9				
MFA	5	0.92	2.0 deg.	3.4
$E_{L(SS)}$	6	0.95	0.7 GPa	4.4
600.0–649.9				
MFA	6	0.95	1.5 deg.	4.3
$E_{L(SS)}$	6	0.95	0.8 GPa.	4.3
650.0–699.9				
MFA	7	0.97	1.2 deg.	5.4
$E_{L(SS)}$	6	0.94	0.9 GPa	4.1

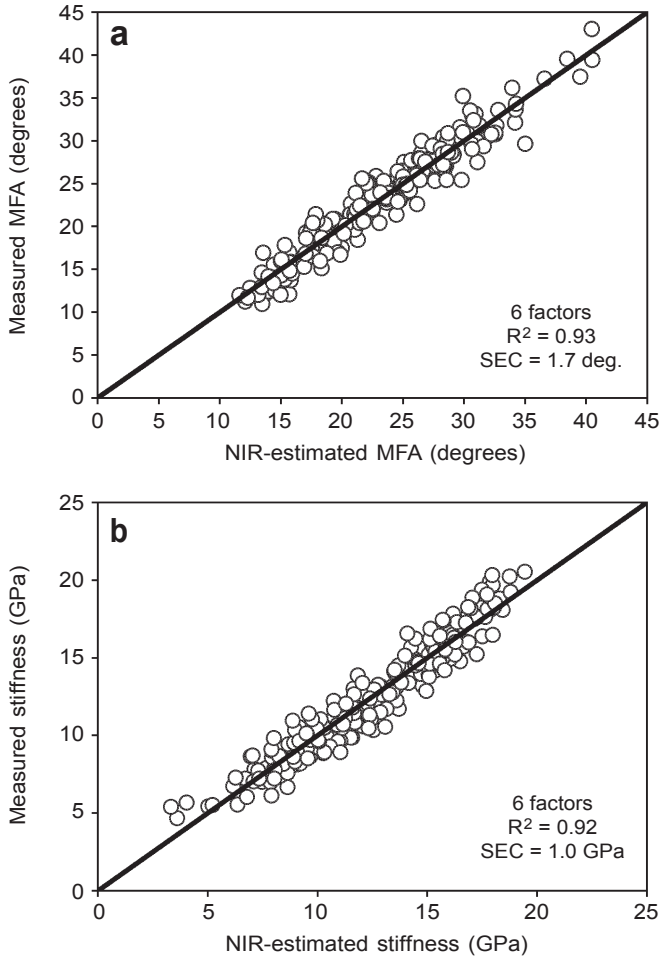

Fig. 1. Relationships between measured values and NIR-estimated values for (a) microfibril angle (MFA) and (b) SilviScan-2 determined stiffness ($E_{L(SS)}$). 229 *Pinus taeda* samples with a density range of 600–699.9 kg/m^3 were used to develop the calibrations.

MFA and $E_{L(SS)}$ calibrations obtained using sets with a density range of 100 kg/m^3 gave poor results when densities were less than 500 kg/m^3. For sets having densities greater than 500 kg/m^3 MFA calibrations improved with increasing density, as shown by an improvement in RPD, while RPD's for the $E_{L(SS)}$ calibrations decreased slightly. MFA and $E_{L(SS)}$ calibrations obtained using densities in the range 600–699.9 kg/m^3 are shown in Figure 1 and demonstrate that data for both parameters were very well fitted.

The 700–799.9 kg/m^3 MFA calibration had two samples with MFA (33.3 and 34.1°) noticeably higher than that for the remaining 81 samples in the set and which could have had a large influence on the calibration statistics obtained for this set. When these samples were deleted a strong calibration for MFA was still obtained (6 factors, R^2 = 0.95, SEC = 1.07°) even though the MFA range was more limited (11.2 to 27.4°).

Strong calibrations for MFA and $E_{L(SS)}$ were obtained when the density range was limited to 50 kg/m^3, provided that density was greater than 500 kg/m^3 (Table 4). The calibrations developed with samples having densities ranging from 550–599.9 kg/m^3 were noticeably better than those obtained using densities ranging from 500–549.9 kg/m^3. MFA calibrations improved as density increased (RPD's continually improved) while $E_{L(SS)}$ calibrations were similar for sets having densities greater than 550 kg/m^3. Relationships between density and MFA and density and $E_{L(SS)}$ were poor (Table 2) for all *P. taeda* sets. The strongest R^2 (0.31) was between density and $E_{L(SS)}$ for the 300–399.9 kg/m^3 set but the majority of *P. taeda* sets had R^2 less than 0.1. Despite the poor relationships it was still possible to obtain strong calibrations for MFA and $E_{L(SS)}$.

The development of MFA and $E_{L(SS)}$ calibrations using 61 *P. taeda* samples with densities limited to 25 kg/m^3 (600.0–624.9 kg/m^3) was investigated. Strong MFA (5 factors, $R^2 = 0.96$, SEC = 1.28°) and $E_{L(SS)}$ (5 factors, $R^2 = 0.96$, SEC = 0.72 GPa) calibrations were still obtained.

The prediction of MFA and $E_{L(SS)}$ using calibrations developed with a narrow density range was also investigated. For example, the *P. taeda* 600–699.9 kg/m^3 samples were split into a calibration (152 samples) and prediction set (77 samples). The calibrations developed for MFA (7 factors, $R^2 = 0.96$, SEC = 1.33°) and $E_{L(SS)}$ (7 factors, $R^2 = 0.95$, SEC = 0.86 GPa) performed well in prediction though predictive errors (MFA, R^2 = 0.87, SEP = 2.12° and $E_{L(SS)}$, $R^2 = 0.85$, SEC = 1.35 GPa) were noticeably higher than calibration errors.

The relationship between PLS factors, MFA and $E_{L(SS)}$

When PLS calibrations are developed, factors are obtained from the NIR spectra that explain most of the variation in the data set. For example 5 factors were required to explain 92% of the MFA variation observed in the 550–599.9 kg/m^3 set (Table 4). In this study it was observed that as the density of the set increased the amount of variation explained by the first factor for both the MFA and $E_{L(SS)}$ calibrations increased. For example, the variation explained by the first factor for the 400–499.9 kg/m^3 *P. radiata* MFA calibration was 54% and increased to 72% for the 600–699.9 kg/m^3 MFA calibration. The *P. taeda* set demonstrated similar behaviour with the first factor explaining 41% of the variation for the 300–399.9 kg/m^3 MFA calibration, increasing to 71% for the 600–699.9 kg/m^3 and 700–799.9 kg/m^3 calibration. The calibration that had the greatest explained variance (76%) was the *P. taeda* MFA calibration developed using samples that had densities in the range 600–649.9 kg/m^3.

The loading plots for the 600–699.9 kg/m^3 *P. radiata* and *P. taeda* MFA calibrations are shown in Figure 2. Both plots have large loadings occurring at similar wavelengths but there is considerable variation in terms of the magnitude of the loadings indicating differences in the overall chemistry of the sample sets. In addition the *P. taeda* plot shows larger loadings than the *P. radiata* plot. Examination of loadings plots for other *P. taeda* sets showed that the loadings were consistently larger than the equivalent *P. radiata* set and may be a consequence of the diverse origins of the *P. taeda* samples.

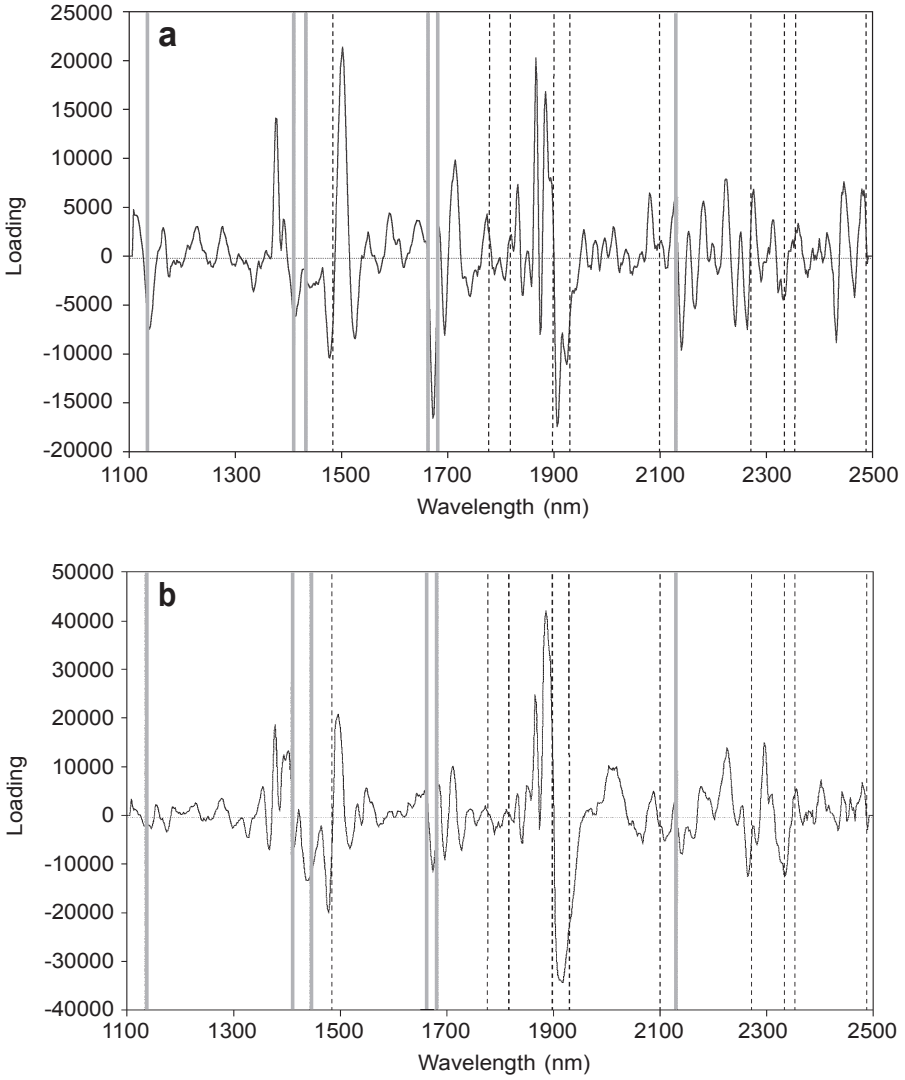

Fig. 2. Loadings plots for the first PLS factor obtained for (a) the *Pinus radiata* microfibril angle (MFA) and (b) the *P. taeda* MFA calibrations. The density range of both sets was limited to 600–699.9 kg/m^3. The variance explained by the first PLS factor was 72% for the *P. radiata* MFA calibration and 71% for the *P. taeda* MFA calibration. Bands that have aromatic origins are indicated by the solid grey lines while the broken lines indicate bands assigned to cellulose.

The plots shown in Figure 2 both have large loadings close to spectral bands assigned to cellulose bond vibrations (Shenk *et al.* 1992; Osborne *et al.* 1993). Particularly noticeable are the strong loadings close to 1490 nm (O-H stretch first overtone) and 1930 nm (O-H stretch / HOH deformation combination). Many strong loadings were also observed in regions of the NIR spectrum whose bands have aromatic origins (lignin and

extractives) (Shenk *et al*. 1992; Osborne *et al*. 1993). Shenk *et al*. (1992) and Osborne *et al*. (1993) did not list bands at 1668, 2084 and 2132 nm but Michell and Schimleck (1996), in a study of wood from *Eucalyptus globulus* Labill., noted that these bands were all very well correlated with hot water extractives and lignin content.

The loadings plots for MFA and $E_{L(SS)}$ were observed to be the inverse of each other for all density groups but in general the magnitudes of the loadings were greater for the MFA calibrations. MFA and $E_{L(SS)}$ are strongly negatively correlated for the sample sets used in this study (Tables 1 & 2), i.e. as MFA decreases (at a constant density) $E_{L(SS)}$ increases, thus explaining why the plots were the inverse of each other.

DISCUSSION

Results presented in this study demonstrate that it is possible to obtain MFA and $E_{L(SS)}$ calibrations using sample sets in which the density range is small and the relationships between density and MFA and density and $E_{L(SS)}$ are poor. Generally stronger MFA and $E_{L(SS)}$ calibrations were obtained using sets that had densities greater than 500 kg/m^3. Weak calibration statistics were obtained for the *P. taeda* sets that had densities less than 500 kg/m^3. MFA calibrations developed with sets having density greater than 500 kg/m^3 improved as density increased.

The inferior calibration statistics observed for *P. taeda* sets having densities less than 500 kg/m^3 are probably a consequence of high average MFA for these sets and limited MFA and $E_{L(SS)}$ range. Average MFA was the highest for the lowest density sets and steadily decreased as density increased (Table 2). The determination of MFA by the analysis of diffraction patterns becomes more difficult as MFA increases owing to the broadening and weakening of the 002 reflections. As MFA increases, the signal-to-noise ratio in the diffraction patterns decreases, reducing the precision with which MFA can be determined. This reduction in precision contributes to the weakness in the calibrations at high MFA. The range of MFA and $E_{L(SS)}$ variation for sets with densities less than 500 kg/m^3 was often narrower than that observed for sample sets having density greater than 500 kg/m^3. For example, MFA ranges for the 300–399.9 kg/m^3 and 400–499.9 kg/m^3 *P. taeda* sets were 14.8 degrees and 22.9 degrees respectively while the MFA range for the 500–599.9 kg/m^3 set was 29.2 degrees. MFA's for the 600–699.9 kg/m^3 *P. taeda* set ranged from 11.0 to 43.0 degrees which approaches the maximum range of MFA that could be reasonably expected for *P. taeda* as determined by SilviScan. The MFA range of the *P. taeda* 700–799.9 kg/m^3 set was comparable to that for lower density sets but a strong calibration was still obtained because X-ray diffraction more precisely determines MFA when MFA is low. For sets with densities less than 500 kg/m^3 the limited MFA and $E_{L(SS)}$ range exacerbates the problem of decreased precision associated with the determination of large MFA. Based on these observations it is probable that calibrations developed using juvenile wood, which inherently has large MFA (Donaldson 1992; Cave & Walker 1994; Evans *et al*. 1999, 2000), would fail to give strong statistics.

X-ray diffractometric analysis on SilviScan-2 is done with the X-ray beam in the tangential direction, i.e. the MFA of the radial walls of longitudinal tracheids was meas-

ured. There are more pits on the radial walls of longitudinal tracheids and owing to the deviation of microfibrils around the pits the MFA measured by SilviScan-2 can overestimate slightly the average MFA of the wood. Measurements of MFA based on the tangential walls of longitudinal tracheids may give a slightly lower MFA but measurements will still suffer from a reduction in precision at high MFA.

An important aspect in the success of this work is matching the NIR data with the corresponding SilviScan data. In future experiments the size of the NIR window will be decreased. Consequently it will be essential to ensure that the section of wood tested corresponds exactly to the SilviScan data as the radial variation of wood properties, both within-rings and from pith-to-bark, is great.

The MFA and $E_{L(SS)}$ calibrations reported in this study are comparable with those reported in Schimleck and Evans (2002a,b) ($E_{L(SS)}$ 8 factors, $R^2 = 0.97$, SEC = 0.91 GPa; MFA 7 factors, $R^2 = 0.95$, SEC = 1.8 degrees) despite the calibrations being developed with sets that had very limited density variation. If adequate MFA and $E_{L(SS)}$ variation exists, and MFA is low enough to be precisely measured by X-ray diffraction, then strong calibrations for these properties can be obtained. The relationship between MFA and $E_{L(SS)}$ was strong for most sets (Tables 1 & 2); therefore, when density variation is limited, MFA variation is the prime determinant of $E_{L(SS)}$ variation. For the MFA and $E_{L(SS)}$ calibrations developed using all samples (729) the calibration statistics were inferior to those reported in Schimleck and Evans (2002a,b) which may be a consequence of using samples from a wide range of sites.

The underlying relationships that have made it possible to obtain calibrations for MFA and $E_{L(SS)}$ were further investigated in this study. Schimleck *et al.* (2002) suggested that the good MFA calibration statistics they obtained may have resulted from the systematic within-tree variation in a range of associated properties, such as cellulose content. Schimleck and Evans (2002b) presented evidence indicating that variation in cellulose content was an important factor in the success of the MFA calibration. Loading plots (Fig. 2) having strong relationships with MFA and $E_{L(SS)}$ show large loadings close to regions of the NIR spectrum that have been assigned to cellulose, supporting the findings of Schimleck and Evans (2002b).

Several large loadings were also observed in regions of the NIR spectrum associated with lignin and extractives hence it is probable that variation in lignin content between samples is also very important in the success of MFA and $E_{L(SS)}$ calibrations. As cellulose and lignin vary, hemicellulose also varies and it is probable that it also is important. Bands in the NIR spectrum arising from hemicellulose occur very close to those observed for cellulose (Shenk *et al.* 1992; Osborne *et al.* 1993; Via *et al.* 2003). It is therefore possible that hemicellulose variation has contributed to the large loadings observed close to regions assigned to cellulose. Similar band assignments could be expected considering the similarities that exist between the sugar units that form cellulose and hemicellulose.

Strong calibrations for MFA and $E_{L(SS)}$ can be obtained when density variation is limited and when there are no relationships between density and MFA or between density and $E_{L(SS)}$. For the MFA and $E_{L(SS)}$ calibrations to be successful, sufficient variation and precise measurement of these properties is required. The loading plots indicate that

variation in wood chemical components such as cellulose, lignin and possibly hemicellulose may be important for NIR calibrations. Further research is required to examine the relationships between MFA, $E_{L(SS)}$, wood chemistry and the NIR spectrum which will require the detailed characterisation of a large set of samples.

ACKNOWLEDGEMENTS

The authors thank the UGA Wood Quality Consortium for the *P. taeda* sample collection and the Georgia TIP^3 program for funding the SilviScan analysis of the *P. taeda* samples. The authors would also like to thank the UGA Wood Quality Consortium for sample preparation and the SilviScan team for the determination of wood properties. Finally the helpful comments of Dr. Jugo Ilic and Mr. Brian Via regarding the text are acknowledged.

REFERENCES

Cave, I.D. & J.C.F. Walker. 1994. Stiffness of wood in fast grown plantation softwoods: The influence of microfibril angle. For. Prod. J. 44: 43–48.

Donaldson, L.A. 1992. Within- and between-tree variation in microfibril angle in Pinus radiata. N. Z. J. For. Sci. 23: 77–86.

Evans, R. 1994. Rapid measurement of the transverse dimensions of tracheids in radial wood sections from Pinus radiata. Holzforschung 48: 168–172.

Evans, R. 1997. Rapid scanning of microfibril angle in increment cores by x-ray diffractometry. In: B.G. Butterfield (ed.), Microfibril Angle in Wood: 116–139. Proc. IAWA/IUFRO International Workshop on the Significance of Microfibril Angle to Wood Quality, Nov. 1997, Westport, New Zealand. University of Canterbury Press.

Evans, R. 1999. A variance approach to the x-ray diffractometric estimation of microfibril angle in wood. Appita J. 52: 283–289, 294.

Evans, R. 2005. Wood stiffness by X-ray diffractometry. In: D.D. Stokke & L.H. Groom (eds.), Characterization of the cellulosic cell wall. Blackwell Publishing, Ames, Iowa. In press.

Evans, R., M. Hughes & D. Menz. 1999. Microfibril angle variation by scanning x-ray diffractometry. Appita J. 52: 363–367.

Evans, R., S. Stringer & R.P. Kibblewhite. 2000. Variation of microfibril angle, density and fibre orientation in twenty-nine Eucalyptus nitens trees. Appita J. 53: 450–457.

Michell, A.J. & L.R. Schimleck. 1996. NIR spectroscopy of woods from Eucalyptus globulus. Appita J. 49: 23–26.

Nyakuengama, J.G., G.M. Downes & J. Ng. 2002. Growth and density responses to later-age fertiliser application in Pinus radiata D.Don. IAWA J. 23: 431–448.

Osborne, B.G., T. Fearn & P.H. Hindle. 1993. Practical NIR spectroscopy with applications in food and beverage analysis, 2nd Ed.: 29–33. Longman Scientific and Technical, Singapore.

Schimleck, L.R., G.M. Downes & R. Evans. 2003. Estimation of Eucalyptus nitens wood properties by near infrared spectroscopy. Proc. 57th Appita Gen. Conf., May, 2003, Melbourne, Australia, pp. 91–97.

Schimleck, L.R. & R. Evans. 2002a. Estimation of wood stiffness of increment cores by near infrared spectroscopy: the development and application of calibrations based on selected cores. IAWA J. 23: 217–224.

Schimleck, L.R. & R. Evans. 2002b. Estimation of microfibril angle of increment cores by near infrared spectroscopy. IAWA J. 23: 225–234.

Schimleck, L.R., R. Evans & J. Ilic. 2001. Estimation of Eucalyptus delegatensis clear wood properties by near infrared spectroscopy. Can. J. For. Res. 31: 1671–1675.

Schimleck, L.R., R. Evans & A.C. Matheson. 2002. Estimation of Pinus radiata D. Don clear wood properties by near infrared spectroscopy. J. Wood Sci. 48: 132–137.

Shenk, J.S., J.J. Workman Jr & M.O. Westerhaus. 1992. Application of NIR spectroscopy to agricultural products. In: D.A. Burns & E.W. Ciurczak (eds.), Handbook of Near-Infrared Analysis: 385–386. Marcel Dekker Inc., New York.

Via, B.K., T.F. Shupe, L.H. Groom, M. Stine & C.-L. So. 2003. Multivariate modelling of density, strength, and stiffness from near infrared spectra for mature, juvenile and pith wood of longleaf pine (Pinus palustris). J. Near Infrared Spectrosc. 11: 365–378.

Williams, P.C. & D.C. Sobering. 1993. Comparison of commercial near infrared transmittance and reflectance instruments for the analysis of whole grains and seeds. J. Near Infrared Spectrosc. 1: 25–33.

Zobel, B.J. & J.R. Sprague. 1998. Juvenile wood in forest trees: 79–91. Springer-Verlag, Berlin Heidelberg.